molecular pharmaceutics

Article

Cite This: Mol. Pharmaceutics 2019, 16, 3665−3677

pubs.acs.org/molecularpharmaceutics

Half-Life Extending Modifications of Peptide YY_{3-36} Direct Receptor-Mediated Internalization

Esben M. Bech,[†,‡] Anette Kaiser,[§] Kathrin Bellmann-Sickert,[§] Søren S.-R. Nielsen,[‡] Kasper K. Sørensen,[‡] Lisbeth Elster,[†] Nikos Hatzakis,[‡,∥] Søren L. Pedersen,[*,†] Annette G. Beck-Sickinger,[*,§] and Knud J. Jensen[*,‡]

[†]Gubra Aps, Hørsholm, Denmark

[‡]Department of Chemistry, University of Copenhagen, Frederiksberg, Denmark

[§]Institute of Biochemistry, Faculty of Life Sciences, Leipzig University, Leipzig, Germany

[∥]Novo Nordisk Foundation Center for Protein Research, Faculty of Health and Medical Sciences, University of Copenhagen, Frederiksberg, Denmark

Supporting Information

ABSTRACT: Peptide YY_{3-36} (PYY_{3-36}) is an endogenous ligand of the neuropeptide Y_2 receptor (Y_2R), on which it acts to reduce food intake. Chemically modified PYY_{3-36} analogues with extended half-lives are potential therapeutics for the treatment of obesity. Here we show that the common half-life extending strategies PEGylation and lipidation not only control PYY_{3-36}'s pharmacokinetics but also affect central aspects of its pharmacodynamics. PEGylation of PYY_{3-36} inhibited endocytosis by increasing receptor dissociation rates (k_{off}), which reduced arrestin-3 (Arr3) activity. This is the first link between Arr3 recruitment and Y_2R residence time. C16-lipidation of PYY_{3-36} had a negligible impact on Y_2R signaling, binding, and endocytosis. In contrast, C18acid-lipidation minimized endocytosis, which indicated a decreased internalization through non-arrestin-related mechanisms. We propose a temporal model that connects the properties and position of the half-life extender with receptor G_i versus Arr3 signaling bias. We believe that this will be important for future design of peptide therapeutics.

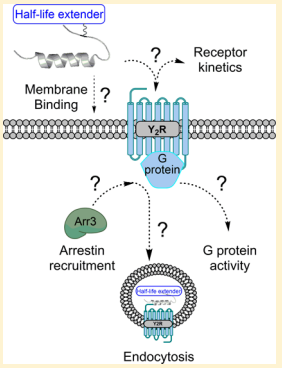

KEYWORDS: *pharmacodynamics, PYY_{3-36}, Y2 receptor, signaling, internalization, lipidation*

INTRODUCTION

Pharmacological doses of peptide YY_{3-36} (PYY_{3-36}) reduce food intake through agonism of the neuropeptide Y_2R receptor (Y_2R), in both lean and obese humans.[1,2] Therefore, PYY_{3-36} analogues show promise as antiobesity biopharmaceuticals.

PYY_{3-36} belongs to the neuropeptide Y (NPY) family, which exerts their biological responses through four rhodopsin-like G protein coupled receptors (GPCRs), Y_1, Y_2, Y_4, and Y_5.[3,4] Full length PYY is released by gastrointestinal L-cells in proportion to food intake,[4] after which it is rapidly truncated into PYY_{3-36} by dipeptidyl-peptidase IV (DPP-IV). From the gut, PYY_{3-36} circulates to the brain to exert its anorectic effects through hypothalamic Y_2 receptors.[5]

Antiobesity pharmaceuticals based on PYY_{3-36} are actively pursued (e.g., refs 6−11), but their development is challenging due to PYY_{3-36}'s insufficient Y_2R selectivity over the other neuropeptide Y family receptors.[12] Moreover, PYY_{3-36} has a short circulatory half-life of ∼10 min,[13,14] like most peptide hormones. Additionally, PYY_{3-36} at supraphysiologic doses elicits dramatic emetic effects (vomiting) in both humans and dogs,[11,15] which partly can be correlated to high peak to trough (lowest concentration between doses) differences in the pharmacokinetic profiles.[11,15] Hence, a stable pharmacokinetic profile is of great importance for future PYY_{3-36}-based pharmaceuticals.

Two widely applied approaches for half-life extension of biopharmaceuticals are PEGylation, the covalent attachment of polyethylene glycol (PEG) chains typically 20−40 kDa in size (PEG20−40),[16] and lipidation, i.e., attachment of fatty acids that bind to albumin and promote self-assembly.[16,17] Both PEGylation and lipidation have been applied to extend the circulatory half-life of PYY_{3-36}.[6,10,11,18,19] However, as for all chemical modifications, PEGylation and lipidation can also affect agonist potency, receptor binding, peptide self-assembly, and *in vivo* distribution.[20−24] Consequently, the effects of PEGylation and lipidation on the pharmacodynamics of PYY_{3-36} and other Y_2R agonists have been difficult to predict. For example, a Y_2R agonist half-life extended through the attachment of a hexadecanoic acid (C16) induced a weight loss in diet-induced obese (DIO) mice that was greater than when the Y_2R agonist was modified with eicosanedioic acid (C20acid) or PEG20 (once daily, 10 nmol/kg, s.c.).[11] This

Received: May 22, 2019
Revised: July 10, 2019
Accepted: July 16, 2019
Published: July 16, 2019

DOI: 10.1021/acs.molpharmaceut.9b00554
Mol. Pharmaceutics 2019, 16, 3665−3677

was surprising, as the C16 modified Y_2R agonist had a much shorter *in vivo* half-life and a lower maximal plasma concentration than the C20acid and PEG20 analogues.[11] However, the C16 attached Y_2R agonist also induced a high degree of emesis in dogs, lessening its clinical potential.[11] This example demonstrates that efficacy and side-effects are not easily balanced in the case of PYY_{3-36} and that they are influenced by *in vivo* half-life and, most likely, several other factors. On the other hand, this provides the opportunity to use lipidation and PEGylation for adjusting the PD properties in a desired direction.

Mäde and colleagues[25] have previously demonstrated how PEGylation and lipidation differentially affected peptide-stimulated receptor internalization. Mäde et al. attached a 22 kDa PEG (PEG22) to the PP analogue Obinepitide which reduced cellular internalization of the peptide and its two primary receptors, Y_2 and Y_4.[25] In contrast, attachment of C16 through a γGlu spacer significantly increased internalization. An important first step in the endocytic process of Y_2R is the recruitment of arrestin-3 (Arr3) to the cytosolic part of the receptor.[3,25] PEG22 and C16-γGlu modification had opposite effects on internalization, which correlated with PEG22 decreasing maximum Arr3 recruitment levels[25] but C16-γGlu increasing it. The intriguing results concerning how C16-γGlu and PEG22 modifications control Arr3 recruitment and internalization of Obinepitide demonstrated a key role of half-life extenders in the control of cellular signaling. However, no mechanistic understanding of the half-life extenders' control was provided, limiting their applicability. To understand the scope of the effects of these chemical modifications, as well as their generality, we chose to study another peptide hormone, PYY_{3-36}, as well as several types of lipidations, and different modification sites in the peptide chain. We studied Y_2R activity, affinity, internalization, and fully characterized Arr3 recruitment. Furthermore, we investigated Y_2R binding kinetics and applied advanced quantitative microscopy to study membrane binding (Figure 1).

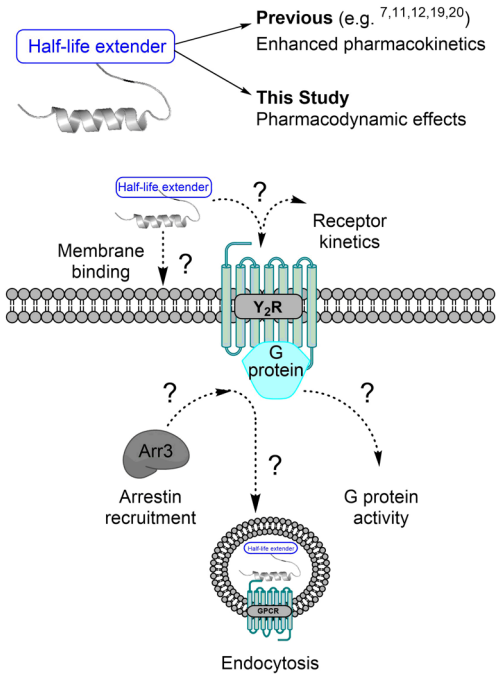

Figure 1. Attachment of half-life extenders to PYY_{3-36} and other peptides enhances pharmacokinetic properties. However, the half-life extending moieties could also affect peptide pharmacodynamics.

MATERIALS AND METHODS

Peptide Synthesis. *Materials.* NHS-ester Atto655 fluorophores were purchased from ATTO-TEC (Siegen, Germany), while mixed isomers of 5 (and 6)-carboxytetramethylrhodamine (TAMRA) were purchased from AAT Bioquest (Sunnyvale, USA). Methoxy-poly(ethylene glycol)-maleimide average molecular weights of 5000 g/mol (PEG5) or 20000 g/mol (PEG20) were acquired from Laysan Bio Inc. (Arab, USA). 18-(*tert*-Butoxy)-18-oxooctadecanoic acid was purchased from BePharm ltd (Shanghai, China). For additional materials, please refer to the Supporting Information.

General. Peptides were assembled using Fmoc-based SPPS, purified by HPLC, and characterized using LC-MS and Maldi-TOF, as described in, e.g., refs 25 and 26. Generally, peptides were modified on resin. However, chemical attachment of large PEG chains and of Atto655-NHS was performed in solution. For detailed information, please refer to the Supporting Information.

***In Vitro* Studies.** *Plasmids.* For BRET studies, two constructs containing the cDNA-sequence coding for human Y_2R C-terminally fused to eYFP and bovine Arr3 N-terminally tagged with *Renilla* luciferase variant 8 (Rluc8) were cloned into pVITRO2-hygro-Mcs (Invivogen) and pcDNA3 (Invitrogen), respectively, as previously described.[25,27,28] For the HA-(hemagglutinin)-tagged hY_2R-eYFP, nine residues (YPYDVPDYA) were added after the initiation codon, and the construct was cloned into pVITRO2-hygro-Mcs (Invivogen).[25] The correctness of all constructs was confirmed by sequencing of the coding region.

Chemocompetent *E. coli* DH5α ($RbCl_2$; NEB, USA) were transformed with the separate plasmids by heat-shock and grown O/N in selective media following the manufacturer's protocol, whereupon the plasmids were purified using a PureYield plasmid midiprep system (Promega, Germany) according to the manufacturer's instructions.

Cell Culture. HEK293 cells were cultured in DMEM/Hams F12 supplemented with 15% heat-inactivated FBS. HEK293_HA_hY2R_eYFP cells were generated, as previously described,[25] through transfection with HA_hY2R-eYFP in pVITRO2-hygro-mcs plasmids and cultured in DMEM/Hams F12 supplemented with 15% heat-inactivated FBS and 0.1% hygromycin. Cell cultivation was performed in a humidified atmosphere at 37 °C and 5% CO_2.

Membrane Preparation. HEK293_HA_hY_2R_eYFP cells were washed and detached in DPBS, 4 °C, after which they were isolated by centrifugation for 5 min at 1800 rpm at 4 °C. The cell pellet was resuspended in 50 mM, pH 7.5, Tris buffer with 50 μM Pefabloc (Sigma-Aldrich), homogenized in a Dounce homogenizer (25× loose pestle, 25× tight pestle), and centrifuged at 2400 rpm at 4 °C for 20 min. Subsequently, the supernatant was transferred to new falcon tubes and centrifuged for 60 min at 12000 rpm at 4 °C. The resulting pellet was resuspended in a 25 mM HEPES buffer (25 mM HEPES, 25 mM $CaCl_2$, 1 mM $MgCl_2$, pH 7.4, with 50 μM Pefabloc) and again homogenized using the Dounce homogenizer before being centrifuged at 12000 rpm at 4 °C for 60 min. Next, the membrane pellet was resuspended in Pefabloc-free HEPES buffer, 4 °C. The protein concentration was determined by Bradford protein assay. Finally, the membrane stock was diluted in the HEPES buffer to 0.3 μg

DOI: 10.1021/acs.molpharmaceut.9b00554
Mol. Pharmaceutics 2019, 16, 3665−3677

of protein/mL, added 50 μM Pefabloc, aliquoted, and stored at −70 °C.

Y_2 Receptor Binding and Kinetic Assay. Y_2 receptor interactions were investigated by competition-based binding assays using isolated membranes from HEK293_HA_-hY_2R_eYFP. Assays were performed in low binding 96-well plates (Greiner Bio-One) with a total volume in each well of 100 μL. ^{125}I-hPYY and cold PYY analogue stock solutions and dilution series were prepared in Milli-Q water with 1% BSA. Y_2R containing membranes were thawed on ice and then diluted to 0.5 μg of protein/40 μL in HEPES buffer (same as above), pH 7.4, with 50 μM Pefabloc (Sigma-Aldrich, Germany) and 1% BSA.

For measurements, to each well was added 10 μL of 600 pM radioligand solution, then 50 μL of cold ligands in varying concentrations (10 μL in kinetic binding experiments), and finally 40 μL of membrane solution (80 μL containing 0.5 μg of protein in kinetic binding experiments). Samples were then incubated at room temperature for 3 h (kinetic measurements: time as indicated) while shaking (200 rpm) before separating the bound ^{125}I-hPYY fraction from the unbound fraction. This separation was performed using a MicroBeta 96-well filtermate harvester (PerkinElmer) to filtrate the solutions through a GFC filter (PerkinElmer) presoaked with 0.1% polyethylenimine (Sigma-Aldrich). Membranes were washed three times with cold PBS and dried for 15 min at 55 °C. Finally, MeltiLex scintillation sheets (PerkinElmer) were melted on the membranes, and radioactivity was quantified using a MicroBeta scintillation counter (PerkinElmer). Unspecific binding was subtracted, and the data were analyzed with GraphPad Prism version 7.03 (GraphPad Software) using the equation "one-site-fit Ki", the determined radioligand concentration used in the assay, and the K_D of the radioligand for Y_2R (50 pM), which has been reported previously.[29] The kinetic data were analyzed using the function "kinetics of competitive binding" with K1 constrained to 6.4e8 M^{-1} s^{-1} (k_{on}, radioligand) and K2 constrained to 0.015 s^{-1} (k_{off}, radioligand, weighted mean of fast and slow phase) as determined previously.[29] K3 (k_{on}, competitor) and K4 (k_{off}, competitor) were fit simultaneously using a global (shared) fit for each peptide. The kinetic K_i was then determined by the ratio of K4/K3.

Y_2 Receptor Activation Assay. Y_2 receptor G protein activities of PYY_{3-36} and its analogues were determined using the Cisbio HTRF cAMP assay Kit optimized for G_i coupled receptors (#62AM9PEC, Cisbio), following the instructions of the manufacturer. Briefly, cAMP was measured by a time-resolved fluorescence technique on the basis of a competitive immunoassay using cryptate-labeled anti-cAMP antibody and d2-labeled cAMP. In the absence of cellular cAMP, the anti-cAMP cryptate conjugate may get into proximity with the cAMP-d2 conjugate and energy (FRET) can be transferred from cryptate to d2. A 384-well assay format with a total assay volume of 20 μL was applied. 2.000 hY_2R expressing CHO-K1 cells (#ES-352-C 22-3-2017, Lot # 460-167-A, stable clonal cell line, PerkinElmer) were incubated with peptide agonists and a fixed concentration of forskolin (~90% forskolin activity) for 40 min at 37 °C using DPBS containing 0.5 mM IBMX as stimulation buffer. After the addition of HTRF detection reagents and incubation for 1 h on a plate shaker (2400 rpm), signals at 620 and 665 nm (raw counts: ratio of 665/620) were detected by a ClarioStar (BMG Labtech) plate reader. Each peptide was tested in at least three separate experiments.

Bioluminescence Resonance Energy Transfer Assay. HEK293 cells were grown to 80−90% confluency in 75 cm^2 flasks and transfected O/N with 11725 ng of pVITRO-hY2R-eYFP and 250 ng of pcDNA3-Arr3-Luc using the transfection agent Metafectene Pro (Biontex) according to the manufacturer's protocol. The next day, cells were reseeded into poly-D-lysine coated white Cell-star (chimney) 96-well plates (Greiner Bio-One) with approximately 150.000 cells/well and incubated O/N. Then, 45 min prior to the BRET measurements, the cell medium was replaced with 100 μL of BRET assay buffer (25 mM HEPES in HBSS pH 7.2). Just prior to the BRET measurements, to each well was added 50 μL of 16.8 μM Coelenterazine H (DiscoveRx) in BRET assay buffer, followed by addition of 50 μL of peptide solution (BRET assay buffer with ≤0.4% DMSO). Measurements were performed using a Tecan Infinite M200 microplate reader using filter sets Blue1 (luminescence 370−480 nm) and Green1 (fluorescence 520−570 nm) at 37 °C. Measurements were performed 5, 15, and 30 min post peptide stimulation. No significant differences were observed between measurements taken 15 and 30 min post treatment. Measurements of 15 min were used for calculations of Arr3 recruitment. Each peptide was tested in at least three separate experiments.

Live-Cell Fluorescence Microscopy. Fluorescence microscopy on live HEK293_HA_hY_2R_eYFP cells was used to examine Y_2R-mediated internalization of Atto655- or TAMRA-tagged PYY_{3-36} analogues. HEK293_HA_hY_2R_eYFP cells were seeded onto μ-Slide 8-wells (Ibidi) to full confluency in 300 μL of DMEM/Hams F12 supplemented with 15% heat-inactivated FBS and 0.1% hygromycine. On the day of the imaging, fully confluent cells were starved for 30 min in Opti-MEM containing Hoechst33342 (Sigma-Aldrich) for nuclei staining. To visualize peptide and Y_2R-eYFP internalization, cells were stimulated with 100 nM fluorescently tagged peptide analogues in Opti-MEM for 60 min. Subsequently, the peptide solution was aspirated, and cells were washed to remove noninternalized peptide. Washing consisted of 1 × 200 μL of HBSS, 1 × 200 μL of acetic wash (50 mM glycine (Serva) and 100 mM NaCl, adjusted to pH 3.1 with glacial acetic acid) for 20 s, and then 1 × 200 μL of HBSS. Finally, 200 μL of Opti-MEM was added to the cells.

Fluorescence microscopy was performed using a Zeiss Axio Observer.Z1 inverted microscope (filters: 46, 02, 31, 50) equipped with an ApoTome Imaging System and a Heating Insert P Lab-Tek S1 unit, as described by Böhme et al. (2008).[27] Each peptide was tested at three or more separate occasions.

Live-Cell Imaging Data Analysis. Following live-cell internalization experiments, images (13−15 per Atto655 peptide containing 44 ± 7 (S.D.) individual cells and 12−29 per TAMRA peptide containing 25 ± 11 (S.D.) individual cells) were exported to ImageJ v.1.5 and analyzed. The cellular internalization of the fluorescently labeled peptides was quantified in ImageJ. Moreover, Y_2R-eYFP internalization was measured by quantification of Y_2R-eYFP colocalized with the fluorescently labeled peptides. Analysis of peptide- and Y_2R-eYFP internalization comprised a script-based identification of cells, disqualification of background and artifact signals, quantification of fluorescence intensity, and estimate of peptide/Y_2R colocalization (Supporting Information Figure S4). The script was coded in Python but applied only tools available in ImageJ v.1.5. The script is in the Supporting Information. Following quantification, internalization degrees

DOI: 10.1021/acs.molpharmaceut.9b00554
Mol. Pharmaceutics 2019, 16, 3665−3677

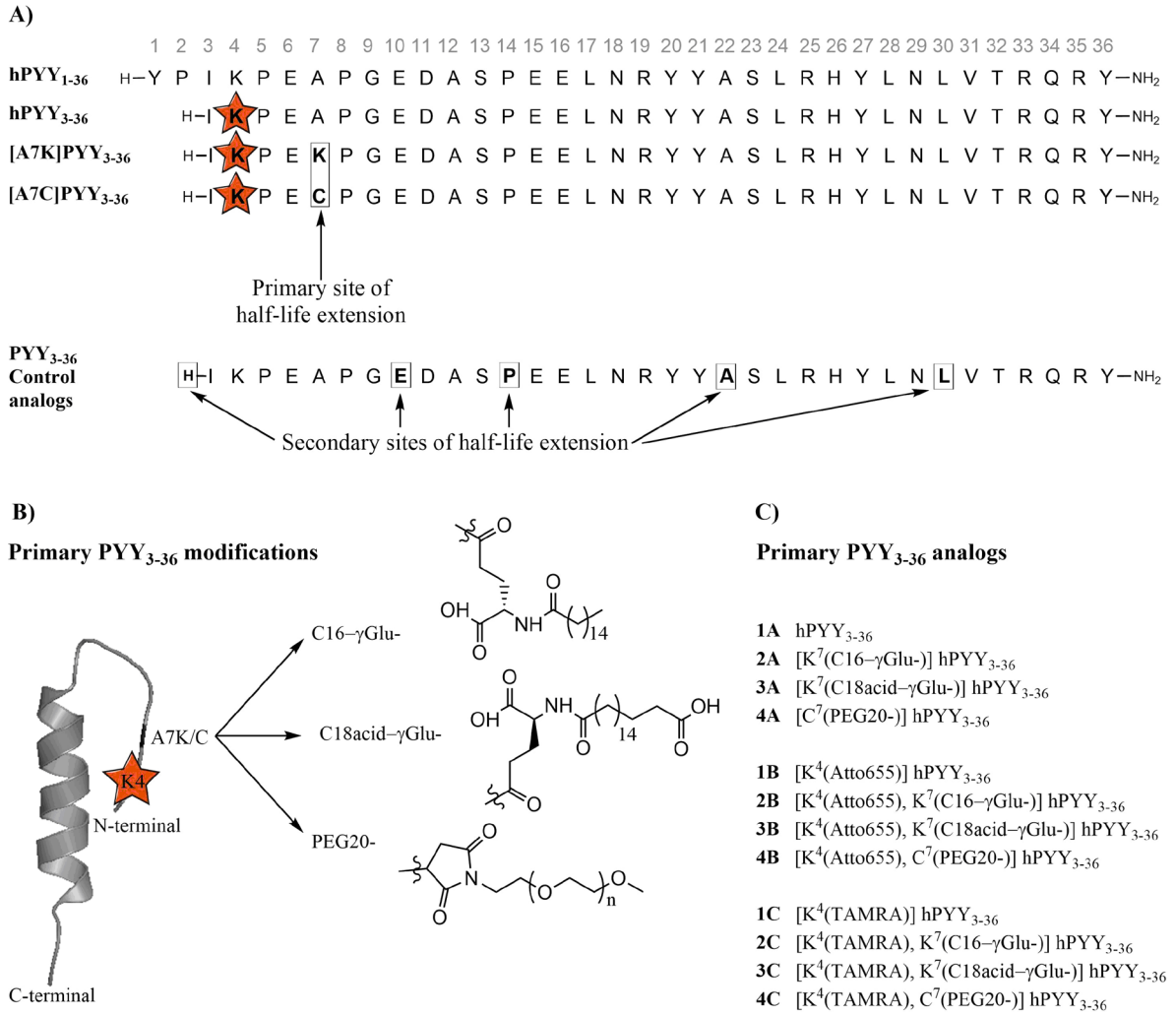

Figure 2. Primary PYY_{3-36} analogues synthesized for this project. (A) Sequences of human PYY_{1-36}, PYY_{3-36}, and the backbones of the primary PYY_{3-36} analogues. Moreover, the modification sites of the control compounds are marked. (B) Crystal structure of native PYY_{3-36} (PDB entry 2DM0[36]) with the primary modifications marked. The star indicates the addition of a fluorophore (Atto655 or TAMRA). (C) Numbering of PYY_{3-36} analogues of primary interest.

were compared using one-way ANOVA analysis with Dunnett's multiple comparisons post hoc test in Prism 7.03.

Membrane Binding; Widefield Microscopy. Liposomes consisting of a 20:29.5:0.5:20:29:1 mixture of cholesterol, 1,2-dioleoyl-*sn*-glycero-3-phosphoethanolamine (DOPE), 1,2-dioleoyl-*sn*-glycero-3-phospho-L-serine (DOPS), 1,2-dioleoyl-*sn*-glycero-3-phosphocholine (DOPC), and 3,3′-dioctadecyloxacarbocyanine perchlorate (DiO, for visualization), which makes up the main components of HEK293 cells,[30] were tethered to passivated microscopy glass slides following our recently developed methodology.[31] Widefield microscopy was then used to visualize the interactions of peptides with liposomes. The liposomes, having nanoscale dimensions, appeared as diffraction-limited dots in an optical microscope. However, the total integrated intensity of a liposome's homogeneously labeled membrane is proportional to the square of its diameter, and we recently showed[32] how this can be used to calculate the diameter of liposomes with very high accuracy (±5 nm).

After gentle washing of the chamber with HBSS, 100 nM peptides **1B**–**4B** were added individually and allowed to equilibrate for 20 min prior to imaging. We calculated the amount of bound peptide to each individual nanoscale liposome by integrating the signal of the Atto655 channel after background correction. To extract densities of bound peptides, peptide signals were normalized to the size of the liposome.[32] All calculations were performed using a script, which is available in the Supporting Information. Finally, densities of bound peptides were transferred to Prism 7.03 and compared using one-way ANOVA with Tukey's multiple comparisons post hoc test.

RESULTS

Design of PYY_{3-36} Analogues. From PYY_{3-36}, a series of half-life extended analogues were created, **2A**–**14A** (Figure 2, Table 1). Of these, particular attention was given to the analogues having C16-γGlu (**2A**), C18acid-γGlu (**3A**), or PEG20 (**4A**) at PYY_{3-36} position 7. Position 7 was selected as the site of modification, as it can be extensively modified with minimal loss of functional activity.[6−8] For the lipidated analogues, a γ-glutamic acid (γGlu) spacer was incorporated between the fatty acid and peptide moieties, as this is known to enhance albumin binding and solubility of many lipidated peptides.[20,33−35] To allow for visualization and quantification

DOI: 10.1021/acs.molpharmaceut.9b00554
Mol. Pharmaceutics 2019, 16, 3665−3677

Table 1. Structure−Activity Relationship for PYY_{3-36} Analogues 1A−14A[a]

	N-term modification	pos. 7	pos. 10	pos. 14	pos. 22	pos. 30	G_i EC_{50} ± SD (nM)	Arr3 EC_{50} ± SEM (nM)
				Primary Peptides				
1A		A	E	P	A	L	0.2 ± 0.1	63 ± 6
2A		K(C16-γGlu-)	E	P	A	L	0.7 ± 0.2	70 ± 17
3A		K(C18acid-γGlu-)	E	P	A	L	0.3 ± 0.2	65 ± 9
4A		C(PEG20)	E	P	A	L	0.9 ± 0.1	2449 ± 308
				Control Peptides				
5A		C(PEG5)	E	P	A	L	0.5 ± 0.2	633 ± 85
6A		K(C18-γGlu-)	E	P	A	L	1.2 ± 0.6	60 ± 2
7A		K(C18acid-)	E	P	A	L	0.5 ± 0.2	88 ± 38
8A	C18acid-γGlu-	A	E	P	A	L	1.4 ± 0.5	992 ± 221
9A		A	K(C18acid-γGlu-)	P	A	L	0.6 ± 0.3	74 ± 19
10A		A	E	K(C18acid-γGlu-)	A	L	0.9 ± 0.1	177 ± 15
11A		A	E	P	K(C18acid-γGlu-)	L	0.6 ± 0.1	158 ± 5
12A		A	E	P	A	K(C18acid-γGlu-)	0.6 ± 0.3	447 ± 127
13A		K(C18acid-γGlu-)	K(C18acid-γGlu-)	P	A	L	2.5 ± 1.6	352 ± 60
14A		K(C18acid-γGlu-)	E	P	A	K(C18acid-γGlu-)	2.3 ± 1.3	1102 ± 321

[a]"G_i EC_{50}" indicates functional hY_2R G_i protein potency characterized in CHO-K1 cells by detecting cAMP levels. "Arr3 EC_{50}" indicates the potency by which peptides recruit arrestin-3 to hY_2R characterized using BRET in HEK293 cells transiently expressing hY_2R-eYFP and Arr3-luciferase. Average G_i and Arr3 EC_{50} values are derived from EC_{50} values calculated in at least three independent experiments with triplicate or duplicate measurements.

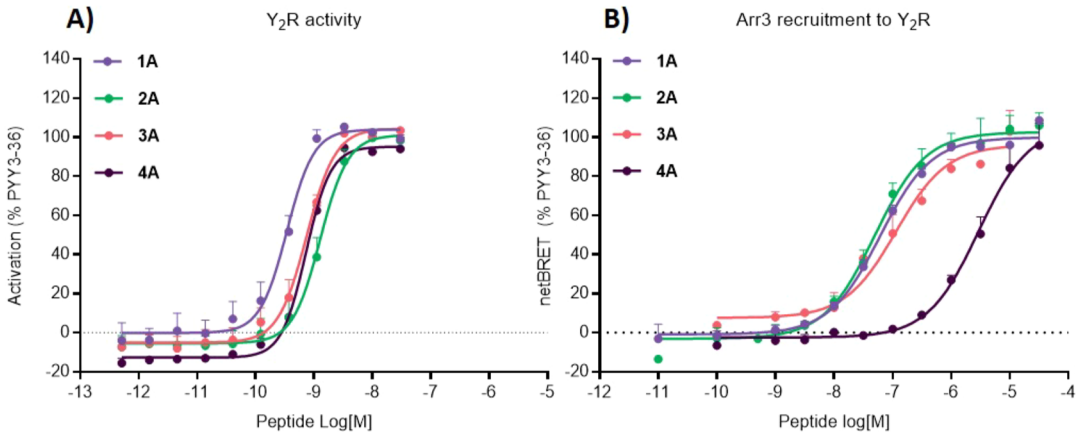

Figure 3. Y_2R signaling upon stimulation of NPY, PYY_{3-36}, or analogues of PYY_{3-36}. (A) hY_2R G_i activity characterized in CHO-K1 cells detecting cAMP levels. (B) Arrestin recruitment to hY_2R stimulated by PYY_{3-36} analogues characterized using BRET in HEK293 cells transiently expressing hY_2R-eYFP and Arr3-luciferase. Curves are examples of one of three individual experiments with each data point measured in duplicates. Error bars illustrate the SEM.

of internalization in living cells, fluorophores (Atto655 or TAMRA) were incorporated at the ε-amine of Lys-4, resulting in peptides **1B−4B** (Atto655) and **1C−4C** (TAMRA). Atto655 is spectrally distinct from eYFP (red and yellow, respectively), which is fused to Y_2R for quantification of the receptor. Thus, the bleed through should be minimal. Atto655 and TAMRA are dissimilar in terms of structure and fluorescence properties. Consequently, application of both types of fluorophores should minimize the likelihood of potential artifacts obscuring results. Finally, to further investigate the effects of PEG size, spacing, lipidation type, lipidation position, and dual lipidation, a set of control peptides were synthesized (**5A−14A**). PEG5 conjugated **5A** was further modified with TAMRA (**5C**) to relate its internalization to that of peptide **4C**. See Table 1 and Supporting Information Table S1 for a full overview of all synthesized analogues.

Half-Life Extenders Differentially Directed Y_2R G_i Activity and an Arr3 Recruitment. GPCR signaling bias can modulate internalization.[37] Hence, the half-life extended PYY_{3-36} analogues were investigated for hY_2R bias in two signaling pathways, G protein activation and arrestin recruitment. G protein activity (G_i) was characterized in CHO-K1 cells using a commercially available kit to detect cAMP levels. Arrestin recruitment to the Y_2 receptor was characterized in HEK293 cells transiently expressing Y_2R-eYFP and Arr3-luciferase using bioluminescence resonance energy transfer (BRET). We chose to study Arr3, rather than arrestin-2, as it is the main driver of Y_2R internalization in HEK293 cells.[38]

With respect to G_i activity, peptides **2A−4A** were full agonists of Y_2R with potencies similar to native PYY_{3-36} (**1A**) (Table 1, Figure 3A). Hence, C16-γGlu, C18acid-γGlu, and PEG20 were incorporated in position 7 of PYY_{3-36} with modest or negligible impact on Y_2R G protein activity.

DOI: 10.1021/acs.molpharmaceut.9b00554
Mol. Pharmaceutics 2019, 16, 3665−3677

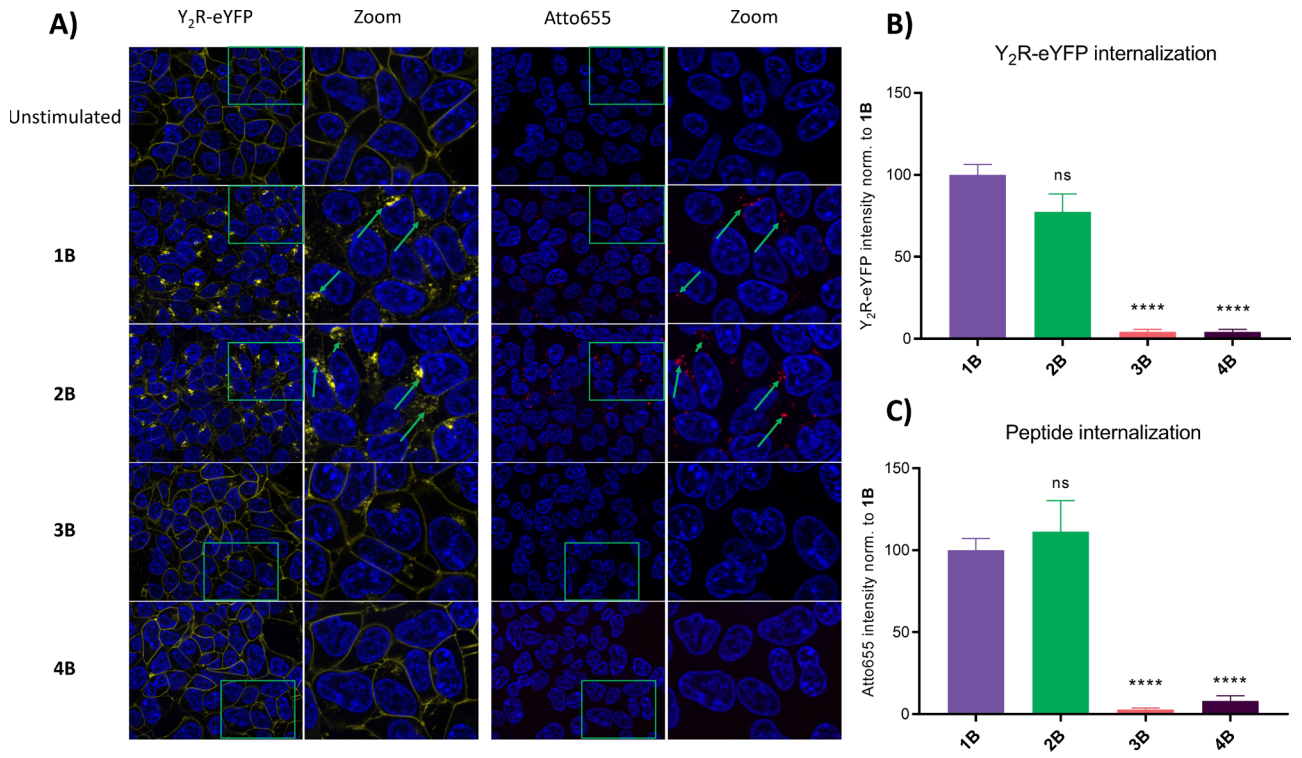

Figure 4. Y_2R Internalization stimulated by Atto655-tagged PYY_{3-36} analogues. Live-cell fluorescence microscopy of HEK293 cells expressing hY_2R-eYFP after 1 h of stimulus with 100 nM **1B**–**4B**. (A) Live-cell images displaying the cell nuclei in blue as well as hY_2R-eYFP (left-most columns) or **1B**–**4B** (right-most columns). (B) Agonist-stimulated Y_2R-eYFP endocytosis normalized to **1B**-stimulated internalization. (C) Intracellular Atto655 intensity normalized to **1B** intensity. Internalization data derives from 13 to 15 image averages per peptide. These images were obtained from three separate experiments, and each image contained 44 ± 7 (S.D.) individual cells. Statistics: Asterisks represent *P*-values below or equal to 0.0001 derived from a one-way ANOVA against **1B** with Dunnett's post hoc test. Error bars represent the SEM.

In contrast, the type of half-life extender had different effects on Y_2R arrestin recruitment and thus Y_2R signaling bias of PYY_{3-36} (Table 1, Figure 3B). PEGylation had a size-dependent impact on Arr3 recruitment (Table 1). Modifying PYY_{3-36} with a 5 or 20 kDa PEG chain (**5A** and **4A**) led to 10-fold and 41-fold, respectively, reduced hY_2R Arr3 recruitment potency (Arr3: **1A**; 60 nM, **4A**; 2449 nM, **5A**; 633 nM). Hence, PEGylation biased PYY_{3-36} signaling toward G protein activity through a reduction of Arr3 recruitment potency. In contrast, addition of C16-γGlu (**2A**) or C18acid-γGlu (**3A**) to PYY_{3-36} did not affect Arr3 recruitment, as compared to the native peptide (**1A**) (Figure 3B).

To address whether PYY_{3-36} lipidation as a rule negligibly affected Y_2R signaling, as observed for analogues **2A**–**3A**, lipidation was investigated in more detail (Table 1). For this, PYY_{3-36} analogues **6A**–**14A** were subjected to the Y_2R G_i activity and Arr3 recruitment assays. Like C16-γGlu and C18acid-γGlu lipidation of PYY_{3-36} position 7, addition of octadecanoic acid-γGlu (C18-γGlu-, **6A**) had little effect on Y_2R signaling, albeit slightly reducing G_i activity. Moreover, the γGlu spacer did not appear to affect Y_2R signaling, as demonstrated by peptide **7A**. Furthermore, addition of C18acid-γGlu at different positions along the midsection of PYY_{3-36} (**9A**–**11A**) was well tolerated in terms of both G_i activity and Arr3 recruitment. Even dual lipidation in the middle region of PYY_{3-36} was relatively well tolerated. Peptide **13A**, lipidated with C18acid-γGlu in both positions 7 and 10, was fully efficacious in both the G_i activity and Arr3 recruitment assays, albeit with a 6- and 12-fold decrease of potency, respectively. While lipidation of PYY_{3-36} in the middle region was well tolerated, lipidation in the N-terminal (**8A**) or position 30 (**12A**) resulted in partial Arr3 recruitment agonism. Both **8A** and **12A** reached only approximately 80% of PYY_{3-36}'s maximal efficacy in the Arr3 recruitment assay (Supporting Information Figure S1). Similarly, dual lipidated peptide **14A**, modified with C18acid-γGlu in both positions 7 and 30, was found to reach just 59% of PYY_{3-36}'s maximal efficacy in the Arr3 recruitment assay (Supporting Information Figure S1). Additionally, **8A**, **12A**, and **14A** all exhibited further reductions in their Arr3 recruitment potencies as compared to their G_i potencies. Hence, if positioned at the N-terminal or near the C-terminal, lipidation of PYY_{3-36} could bias Y_2R signaling toward the G protein pathway and away from the Arr3 pathway, and dual lipidation could enhance this bias. However, lipidation along the midregion yielded fully efficacious, unbiased analogues with negligible reductions in potencies.

Half-Life Extenders Differentially Directed Internalization of PYY_{3-36} and Y_2R in Living Cells. With the aim to directly observe Y_2R internalization synchronously with PYY_{3-36} docking, HEK293 cells overexpressing hY_2R-eYFP were incubated with PYY_{3-36} analogues tagged with either Atto655 (**1B**–**4B**) or TAMRA (**1C**–**5C**). Peptide labeling generally resulted in a relatively modest decrease in activity (Supporting Information Table S1). As an exception, the PEG20 modified **4C** was found to have a Y_2R G_i potency 100-fold lower (44 nM) than the TAMRA-tagged native-like peptide, **1C**. For the agonist-stimulated internalization experiments, the HEK293 cells were incubated for 1 h with 100 nM of all peptides except **4C**, which was added in a concentration

DOI: 10.1021/acs.molpharmaceut.9b00554
Mol. Pharmaceutics 2019, 16, 3665–3677

Table 2. Y_2 Receptor Binding Kinetics and Affinities of PYY_{3-36} and Half-Life Extended Analogues[a]

peptide	position 7 modification	other modifications	k_{on} ± SD (M^{-1} min^{-1})	k_{off} ± SD (min^{-1})	K_i (nM)	K_i* (nM)
			Primary Peptides			
1A (PYY_{3-36})			$8.4 \times 10^7 \pm 2.7 \times 10^7$	0.06 ± 0.03	0.7	1.3
2A	K7(C16-γGlu-)		$5.2 \times 10^7 \pm 3.4 \times 10^7$	0.10 ± 0.08	2.0	1.5
3A	K7(C18acid-γGlu-)		$1.2 \times 10^7 \pm 0.6 \times 10^7$	0.07 ± 0.04	5.7	5.9
4A	C7(PEG20-)		$13.4 \times 10^7 \pm 3.0 \times 10^7$	0.68 ± 1.6	5.1	17.6
			Control Peptides			
5A	C7(PEG5-)		ND	ND	ND	13.7
7A	K7(C18acid-)		ND	ND	ND	4.0
8A		C18acid-γGlu-[Nt]	ND	ND	ND	114.4
12A		K30(C18acid-γGlu-)	ND	ND	ND	46.1
14A	K7(C18acid-γGlu-)	K30(C18acid-γGlu-)	ND	ND	ND	649.9

[a]The association (k_{on}), dissociation (k_{off}), and dissociation equilibrium constant (K_i) derived from four independent competition-based kinetic Y_2R assays with triplicate measurements. K_i* derives from two to three independent Y_2R heterologous equilibrium saturation assays with duplicate measurements.

of 1 μM due to its reduced activity. After incubation, peptide and receptor internalization was analyzed by confocal fluorescence microscopy and quantified using an in-house developed Python script based on ImageJ analysis.

Prior to peptide stimulation, Y_2R-eYFP was localized exclusively in the cell membrane (Figure 4A and Supporting Information Figure S2A). Upon stimulation with 100 nM of the native-like PYY_{3-36} analogues **1B** and **1C**, the receptors largely relocalized to the vesicular compartments of the cells. Moreover, **1B** and **1C** colocalized with the internalized Y_2R, altogether indicating agonist-stimulated endocytosis. The half-life extended PYY_{3-36} analogues also induced Y_2R internalization, but the degree varied significantly depending on the half-life extender.

Analysis of cells stimulated by Atto655-tagged PYY_{3-36} analogues revealed how the C16-γGlu modified **2B** induced Y_2R-eYFP internalization *on par* with native-like peptide **1B** (Figure 4B). In contrast, peptides modified by C18acid-γGlu (**3B**) and PEG20 induced minimal Y_2R-eYFP internalization compared to treatment with **1B**. As a second method for analysis of internalization, intracellular Atto655 fluorescence was quantified. Again, the C16-γGlu modified **2B** internalized to the same extent as the native-like peptide **1B**, while the remaining Atto655-tagged peptides internalized significantly less (Figure 4C). The fact that both peptide and Y_2R internalize to the same extents strongly supports a peptide-mediated internalization.

As a control to test whether Atto655 labeling had influenced the peptides' Y_2R interactions and the subsequent endocytosis, internalization experiments were also performed with TAMRA labeled peptides (Supporting Information Figure S2). Consistent with the Atto655 experiments, stimulation with native-like peptide (**1C**) or the C16-γGlu modified peptide (**2C**) resulted in a much higher Y_2R-eYFP internalization compared to treatment with C18acid-γGlu (**3C**) and PEG20 (**4C**, 1 μM) modified peptides. Similarly, the PYY_{3-36} analogue modified with PEG5 (**5C**) also promoted negligible Y2R-eYFP internalization. The somewhat higher apparent internalization of peptide **1C** compared to **2C** in Figure S2 could originate from small variation in peptide orientation that, due to the presence of FRET between TAMRA and eYFP, results in a relative TAMRA signal increase. Nonetheless, quantification of intracellular TAMRA signaling confirmed that **1C** and **2C** internalized to a much higher extent than **3C**−**5C**.

In summary, live-cell microscopy revealed how three types of half-life extenders differentially directed internalization of PYY_{3-36} and its receptor. Lipidation of PYY_{3-36} with C16-γGlu led to internalization *on par* with the native ligand. In contrast, lipidation with C18acid-γGlu dramatically reduced internalization. The same holds true for modification with either PEG5 or PEG20.

The Type and Position of a Half-Life Extender Controlled Y_2R Affinity and Kinetics. Recent literature points to a correlation between GPCR endocytosis and the residence time of a ligand at the receptor. Specifically, increasing k_{off} rates have been demonstrated to reduce Arr3 recruitment and, subsequently, internalization.[39−41] We therefore investigated Y_2R binding and kinetics of the half-life extended PYY_{3-36} analogues as a potential basis for their differential Arr3 recruitment and internalization patterns. For this, membranes of HEK293 cells expressing hY_2R-eYFP were isolated and used in two heterologous radioligand binding assay setups, an equilibrium saturation binding assay and a kinetic competition assay. In both cases, ^{125}I-$hPYY_{1-36}$ was used as the radioactive agonist (Table 2).

The heterologous equilibrium saturation assay established hY_2R binding affinities (K_i) against which the kinetic data could be verified. The K_i of native PYY_{3-36} (**1A**) was found to be 1.3 nM. Lipidation of PYY_{3-36} position 7 by C16-γGlu (**2A**) did not affect Y_2R affinity, while addition of C18acid-γGlu to the same position slightly reduced the affinity (**3A**, K_i 5.9 nM). The γGlu spacer applied for both peptides **2A** and **3A** did not importantly contribute to the retained Y_2R affinity of the lipidated PYY_{3-36} analogues, as demonstrated by peptide **7A** (K_i 4.0 nM). However, in some cases, changing the lipidation site had a large effect on the Y_2R binding affinity. Changing the C18acid-γGlu attachment site from position 7 to 10 of PYY_{3-36} did not impact the hY_2R affinity (**8A**, K_i 4.3 nM), while lipidation in the N-terminal or at position 30 increased K_i to 114 and 46 nM, respectively (**8A** and **12A**). Hence, lipid position could greatly affect Y_2R affinity. Finally, PEGylation was found to reduce the Y_2R affinity of PYY_{3-36} in a size-dependent manner, so that PEG20 reduced the binding affinity more than PEG5 (**4A**, K_i 17.6 nM to **5A**, K_i 13.7 nM). In summary, lipidation at position 7 had a modest impact on Y_2R affinity, while the large PEG chains more severely reduced affinity.

The kinetics of **1A**−**4A** binding to hY_2R was studied in a time-varied competitive binding setup (Supporting Informa-

DOI: 10.1021/acs.molpharmaceut.9b00554
Mol. Pharmaceutics 2019, 16, 3665−3677

tion Figure S3). The Y_2R binding kinetics of the C16-γGlu modified PYY_{3-36} analogue **2A** corresponded to those observed for the native peptide (**1A**). Meanwhile, the C18acid-γGlu modified **3A** had a 7-fold reduced k_{on} rate compared to **1A**, resulting in the slightly reduced Y_2R affinity identified for **3A** in the heterologous equilibrium saturation setup. In contrast to the lipidated peptides, the PEGylated PYY_{3-36} analogue **4A** was found to have a markedly increased Y_2R k_{off} rate (11-fold) as compared to native PYY_{3-36} (**1A**).

In summary, the Y_2R binding experiments revealed how both the type and position of a half-life extender affected the receptor affinity and kinetics of the PYY_{3-36} analogues.

Membrane Binding Displays Clear Differences. It is well-known that lipidated peptides often bind to membranes.[42−46] Peptides with amphipathic helices, such as PYY, have been hypothesized to bind to cell membranes as an important first step before binding to receptors.[47−49] This raised the question of whether membrane binding might impact Y_2R kinetics of the PYY_{3-36} analogues, ultimately affecting signaling bias and internalization. We therefore studied the binding of peptides **1B**−**4B** on model nanoscopic membrane lipidic systems, liposomes, with lipid compositions practically identical to the membrane of HEK293 cells (see the Materials and Methods). Liposomes were homogeneously fluorescently labeled with DiO (3,3′-dioctadecyloxacarbocyanine perchlorate) and tethered on passivated surfaces. This allowed us to image them individually[32] and extract their radius with nm precision and their location with subresolution accuracy.[32] Subsequently, incubation with Atto655-tagged PYY_{3-36} analogues permitted an accurate assessment of peptide densities over thousands of liposomes. While liposome populations are polydisperse in size,[32] resolving individual liposomes allowed for a focus on monodisperse liposomes of 50 ± 5 nm. Thus, membrane-curvature-mediated variations in the membrane binding affinity and density of the peptides were minimized.

Membrane binding density correlated with the hydrophobicity of the half-life extending moiety (Figure 5). Compared to the native-like **1B**, C16-γGlu lipidated **2B** showed a doubling of the average membrane binding (**1B** avg. 31 A.U.; **2B** avg. 67 A.U.). This was observed as a reduction of the low-density events and a right-shift in the distribution of bound peptides per liposomes. C18acid-γGlu and PEG20 modified peptides **3B** and **4B** both bound significantly less than **2B**. However, **3B** and **4B** had opposite tendencies with respect to membrane binding. **3B** had a significantly increased membrane binding compared to the PEGylated **4B** (doubled). Overall, data indicated that lipidation with C16-γGlu would greatly enhance PYY_{3-36}'s binding to the cell membrane, while lipidation with C18acid-γGlu would not. Furthermore, PEGylation would reduce interactions of PYY_{3-36} with the cell membrane.

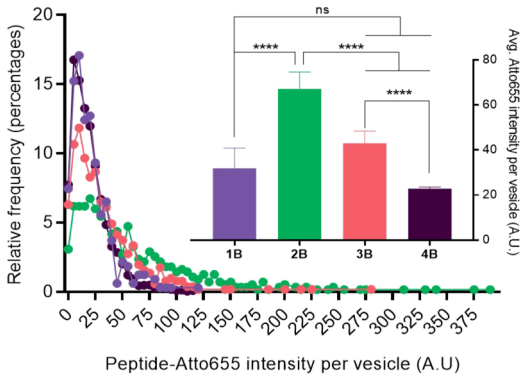

Figure 5. Membrane binding PYY_{3-36} analogues. The normalized frequency of binding of Atto655-tagged PYY_{3-36} analogues (**1B**−**4B**) to surface-adhered DiO-loaded vesicles was visualized by widefield microscopy. Liposomes consisted of the main components of HEK293 cell membranes as well as 1% DiO for visualization (see the Materials and Methods section). 350−3000 liposomes were analyzed per peptide. The scatterplot is a histogram showing the distribution of measurements, where the *Y*-axis is the relative frequency of observations in percentage and the *X*-axis is the background-corrected Atto655 intensity for a vesicle of a fixed size (50 ± 5 nm). Thus, a right-shift in the histogram indicates an increase in membrane-binding events. The inset displays the average peptide fluorescence per vesicle. Statistics: Asterisks represent *P*-values ≤0.0001 derived from a one-way ANOVA against **1B** with Tukey's post hoc test. Error bars illustrate SEM.

DISCUSSION

Attachment of PEG, C16, and C18acid can extend the circulatory half-life of polypeptides, as successfully demonstrated with several marketed peptide pharmaceuticals.[16,17,20,34,50] However, half-life extenders may modify peptide properties beyond pharmacokinetics, i.e., agonist-stimulated endocytosis of GPCRs.[25] This process is observed for many GPCRs and can result in a desensitization of the cell surface and altered receptor signaling.[51] Whether the Y_2R undergoes endocytosis has previously been contested,[52−55] but it is now generally recognized that Y_2R internalizes upon agonist stimulation in an Arr3-dependent fashion.[3,25,27,28,38,56−58] Here, we investigated how PYY_{3-36}-stimulated internalization and signaling of Y2R was affected by C16-γGlu lipidation, C18acid-γGlu lipidation, and PEGylation of the peptide agonist. The main observations are summarized in Figure 6.

In vitro characterization revealed how both the half-life extending moiety and the site of modification governed Y_2R signaling of PYY_{3-36}. In solution, PYY_{3-36} consists of an unstructured C-terminal, a central amphipathic α-helix stretching from residue 15 to 32, and an N-terminal region, which folds back onto and stabilizes the α-helix (Figure 2B).[36,59,60] With respect to Y_2R binding and activation, the C-terminal of PYY_{3-36} is critical,[60,61] but truncations or alterations in the N-terminal and the central helix can also reduce Y_2R affinity.[60] We found that addition of half-life extenders in position 7 of PYY_{3-36} (**1A**−**7A**) was well tolerated with respect to the Y_2R G_i signaling but had different effects on agonist-stimulated Y_2R arrestin recruitment (Table 1). While lipidation of position 7 did not affect PYY_{3-36}-stimulated arrestin recruitment (**2A**, **3A**, **6A**, **7A**), PEGylation dramatically and size-dependently reduced arrestin recruitment. Hence, PYY_{3-36} analogues lipidated at position 7 elicited native Y_2R signaling, while PEGylation biased Y_2R toward G_i signaling in a size-dependent manner. The type of half-life extender but also the site of modification affected the Y_2R signaling. Lipidation of PYY_{3-36} in positions 7, 10, 14, and 22 (**2A**, **3A**, **6A**−**11A**) had negligible effects on its Y_2R G_i activity or Arr3 recruitment. However, repositioning of C18acid-γGlu to the N-terminal or near the C-terminal of PYY_{3-36} reduced its potencies and efficacies in the Arr3 recruitment assay, resulting in Y_2R G_i-biased activities (**8A** and **12A**). Similarly, while dual C18acid-γGlu lipidation of PYY_{3-36} in positions 7 and 30 promoted a G_i bias (**14A**), dual C18acid-γGlu

DOI: 10.1021/acs.molpharmaceut.9b00554
Mol. Pharmaceutics 2019, 16, 3665−3677

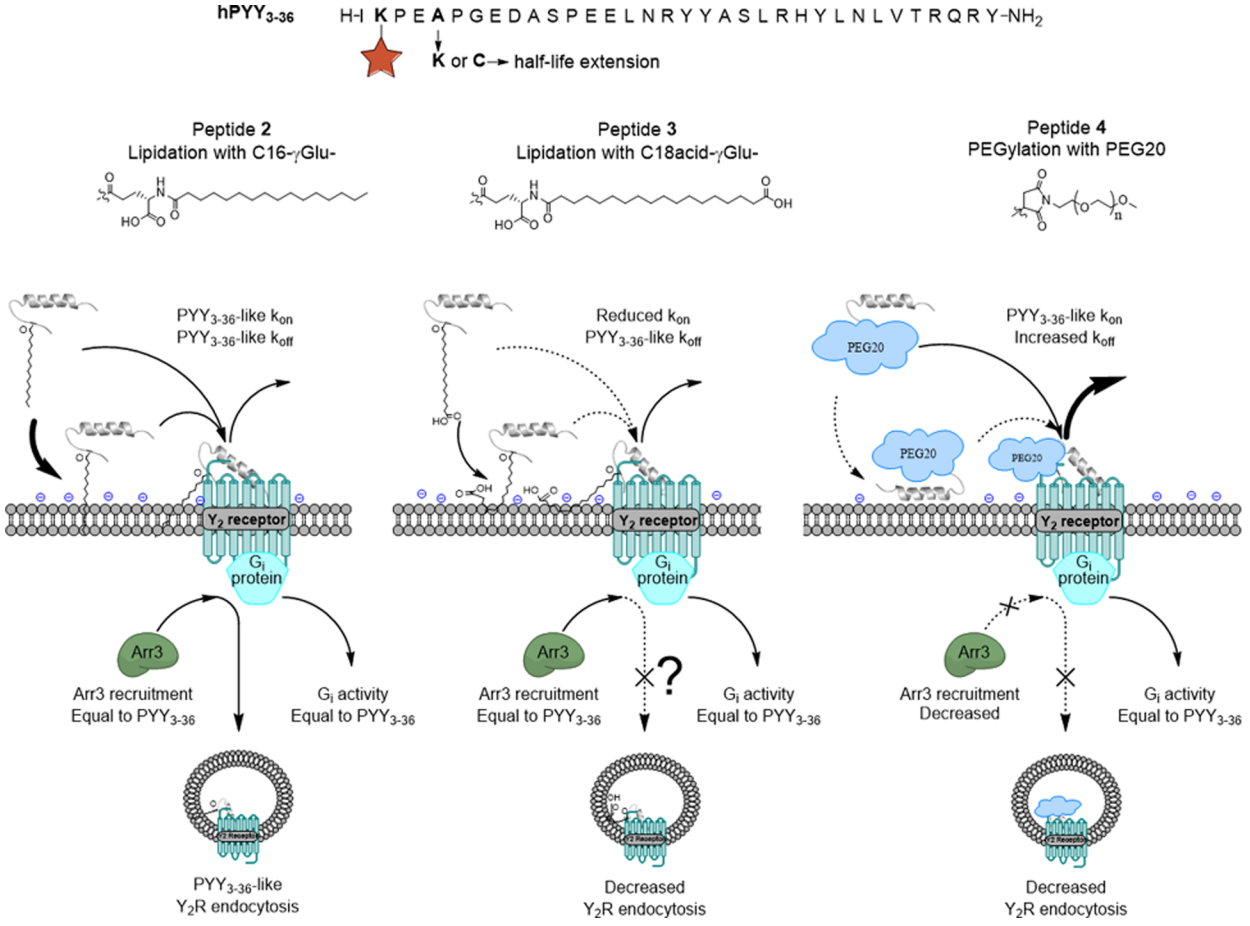

Figure 6. Differential impact of three half-life extenders, C16, C18acid, and PEG20, added to position 7 of PYY_{3-36} (peptides **2**, **3**, and **4**). Thin arrows indicate properties equal to those of PYY_{3-36} (peptide **1**). Increased, reduced, and highly reduced properties compared to PYY_{3-36} are illustrated by bold, dotted, and dotted hashed arrows, respectively. Addition of C16 to PYY_{3-36} increased membrane binding but did not influence Y_2R binding, Arr3 recruitment, G_i activity, or internalization. Addition of C18acid did not impact PYY_{3-36}'s membrane binding, Arr3 recruitment, or G_i activity. However, C18acid slowed the Y_2R association rate (k_{on}) and reduced endocytosis through an unknown mechanism. Addition of a large-chain PEG (peptide **4**) reduced PYY_{3-36}'s membrane binding and increased its Y2R k_{off} rate. The reduced Y_2R residence time did not impact G_i activity but diminished Arr3 recruitment, and thus decreased endocytosis.

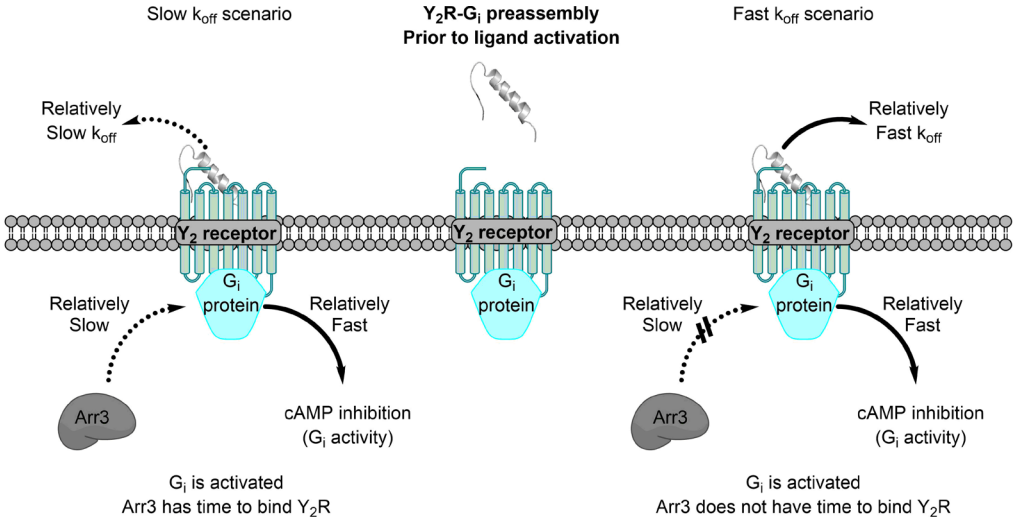

Figure 7. A temporal model showing how ligand residence time at the Y_2R could determine Arr3-G_i signaling bias. Y_2R and its designated G_i protein are preassembled prior to ligand binding. Upon ligand activation of the receptor, the activation of G_i is therefore relatively faster than the recruitment of Arr3. Thus, increasing ligand Y_2R k_{off} can decrease Arr3 recruitment potency without affecting G_i activity.

DOI: 10.1021/acs.molpharmaceut.9b00554
Mol. Pharmaceutics 2019, 16, 3665−3677

lipidation of positions 7 and 10 did not bias Y_2R activity (**13A**). Thus, our studies showed that C18acid-γGlu could bias PYY_{3-36} activity depending on the site of chemical modification. We hypothesize that this could be a general feature also for other lipidation strategies and other peptide hormones.

Live-cell fluorescence microscopy revealed how C16-γGlu, C18acid-γGlu, and PEG20 differentially directed PYY_{3-36}-stimulated Y_2R endocytosis (Figure 4 and Supporting Information Figure S2). In HEK293 cells, **1B** and **1C** induced a marked Y_2R endocytosis. PYY_{3-36} lipidated with C16-γGlu in position 7 (**2B** and **2C**) induced Y_2R endocytosis *on par* with the native-like peptide. In contrast, lipidation of the same position with C18acid-γGlu (**3B** and **3C**) minimized internalization. Thus, despite their relative similarity, the two lipids promoted strikingly different endocytic responses. PEGylation of PYY_{3-36} position 7 reduced Y_2R endocytosis (**4B**, **4C**, and **5C**), similar to C18acid-γGlu lipidation. Our *in vitro* characterization of Y_2R signaling had shown that addition of PEG20 (**4A**) at position 7 of PYY_{3-36} reduced its Arr3 recruitment potency. Arr3 recruitment is an important first step for Y_2R internalization. Thus, the decreased Arr3 response of PEGylated peptides aligned with their reduced internalization (Figure 4 and Supporting Information Figure S2). However, C18acid lipidation of position 7 in PYY_{3-36} (**3**) also minimized internalization, despite having negligible effects on Y_2R G_i activity or Arr3 recruitment. Hence, dissimilar mechanisms governed the reduced internalization of PYY_{3-36} modified by C18acid-γGlu- and PEG. PEGylation decreased internalization through a reduced Arr3 recruitment efficiency, while C18acid-γGlu appeared to decrease internalization through steps different from Arr3 recruitment.

Studies of Y_2R binding kinetics provided a link between Y_2R dissociation rates (k_{off}) and the Arr3 recruitment of the half-life extended PYY_{3-36} analogues. Recent literature suggests a correlation between the kinetics of ligands that bind GPCRs and GPCR endocytosis. Specifically, increasing ligand k_{off} has been found to reduce Arr3 recruitment and, subsequently, endocytosis.[40,41,62,63] In 2018, Kaiser et al.[29] unveiled that Y_2R and its designated heterotrimeric G protein assembles prior to agonist stimulation. On the basis of these findings and observations from our half-life extended PYY_{3-36} analogues, we propose a temporal model in which Y_2R ligands can be biased toward G_i activity by increasing their k_{off} rates (Figure 7). Due to the Y_2R-G_i preassembly, activation of the G protein would be expected to occur rapidly upon Y_2R activation and prior to any Arr3 recruitment. Hence, reducing the time that Y_2R spends in the active conformation after ligand binding would decrease Arr3 recruitment but not necessarily reduce the G_i activity. In the case of our half-life extended PYY_{3-36} analogues, neither lipidation by C16-γGlu nor C18acid-γGlu (**2A** and **3A**) affected Y_2R k_{off}, albeit C18acid-γGlu slightly reduced the k_{on} rate (Table 2). This aligns well with the retained G_i activities and Arr3 recruitment potencies of the lipidated peptides. Meanwhile, PEG20 was found to increase the Y_2R k_{off} rate of PYY_{3-36} approximately 10-fold (**4A**) and to promote a Y_2R G_i bias, which aligns with our temporal model. The low internalization observed for the PEGylated peptides was therefore likely governed by faster Y_2R k_{off} rates.

Next, the membrane binding of the PYY_{3-36} analogues was studied, as it could potentially impact Y_2R receptor binding[47−49] and the dynamics of receptor recycling post-internalization.[64−66] The binding of the PYY_{3-36} analogues tagged with Atto655 (**1B**−**4B**) to vesicles was used as the cell membrane model (Figure 5). The membrane binding of **1B**−**4B** correlated with the general hydrophobicity of the half-life extending moiety. C16-γGlu significantly increased the membrane binding of PYY_{3-36} (**2B**) as compared to the binding at identical concentrations for **1C**. In contrast, lipidation with C18acid-γGlu (**3B**) did not significantly affect PYY_{3-36}'s membrane binding, which can probably be accredited to its distal (omega) negative charge. It can be assumed that the omega end of C18acid cannot penetrate the lipid bilayer because of its carboxylic acid, leaving the middle section for interaction with the lipid bilayer. In contrast to lipidation, PEGylation of PYY_{3-36} (**4B**) reduced the density of peptide bound at the membranes, which correlated with the size of the hydrophilic polymer. The differential degrees of membrane binding promoted by C16-γGlu, C18acid-γGlu, and PEG20 correlated qualitatively to the Y_2R binding affinities of their respective peptide analogues, where **2A** > **3A** ≥ **4A** (Table 2). This could indicate that membrane binding was in fact implicated in the receptor binding of PYY_{3-36}, alongside, e.g., steric hindrance (particularly relevant for the PEGylated peptide). Moreover, these results demonstrated that C18acid-γGlu is less adherent toward hydrophobic surfaces as compared to C16-γGlu. This is interesting, as cell membrane adherence has been hypothesized as one (secondary) mechanism in which lipidation extends peptide half-lives *in vivo*.[17]

The reduced endocytosis of the C18acid-γGlu modified peptide might be explained through the so-called "signaling barcode" model. The barcode model states that ligands can differentially alter the internalization pattern of a GPCR by directing its intracellular conformation.[67] However, such a change would be expected to change the spatial BRET orientation between the receptor and arrestin (eYFP relative to luciferase) and thus the observed absolute (raw) BRET values, as recently demonstrated for chimeric Y_1/Y_2 receptors.[28] No such change was observed for any of the peptides in this study. Instead, we hypothesize that the C18acid may restrict PYY_{3-36}-stimulated Y_2R internalization dynamics by interactions with the extracellular matrix.[58,68] Anionic side chains in Y_2R's N-terminal extracellular segment PDPEPE, located adjacent to the PYY_{3-36} binding pocket, have been shown as a primary factor for the reduced internalization rate of Y_2R compared to the Y_1 receptor.[58,68] The mechanism behind the PDPEPE segment's control of Y_2R internalization rates is unknown, but association between the domain and connector proteins of the extracellular matrix has been suggested to play a role.[58] Aspartate side chains are known to be important for interaction with integrins and other connector proteins, and by mutating the aspartic acid of PDPEPE to an alanine, the Y_2R internalization rate was dramatically increased.[58] We hypothesize that the distal carboxyl group of the C18acid lipidation motif could also interact with extracellular matrix proteins, which might act to slow the rate of internalization. Alternative to this scenario, the different internalization patterns promoted by C16-γGlu and C18acid-γGlu might originate from distinct effects on receptor recycling dynamics. This was recently shown for another GPCR, the neuromedin U2 receptor (NMU2), where intracellular processing and recycling rates depended on the nature of the bound peptide ligand.[66] Like NMU2, Y_2R recycles back to the plasma membrane after ligand stimulation through a highly regulated process that remains incompletely understood.[51] An important step in the

DOI: 10.1021/acs.molpharmaceut.9b00554
Mol. Pharmaceutics 2019, 16, 3665−3677

recycling process is dissociation of the ligand from the receptor in acidified endosomal vesicles.[51,69] The C18acid modification might facilitate a faster ligand release and thus less endosomal accumulation despite showing a strong initial Arr3 interaction.

The Y_2R internalization pattern and signaling bias observed for the C16-γGlu modified PYY_{3-36} (**2A**) is different from what has previously been reported by Beck-Sickinger and colleagues for C16-γGlu modified Obinepitide.[25] This first study found that modification of Obinepitide by C16-γGlu facilitated Arr3 recruitment and, subsequently, internalization, while PEGylation (PEG22) decreased endocytosis.[25] In contrast, our C16-γGlu modified PYY_{3-36} analogue (**2A**) conferred an unbiased Y_2R signaling with a maximal Arr3 recruitment equal to that of the native ligand. Furthermore, our C16-γGlu modified PYY_{3-36} analogue did not increase agonist-stimulated internalization compared to the native peptide. Hence, while PEGylation of PYY_{3-36} and Obinepitide uniformly decreased Y_2R-endocytosis, addition of C16-γGlu increased internalization only in the case of Obinepitide. This difference could be due to differences between the two peptides, or a consequence of C16-γGlu being inserted in position 22 of Obinepitide and position 7 of PYY_{3-36}.

In summary, modifying peptides with half-life extenders can affect their receptor-mediated internalization profiles, their receptor signaling, as well as their biophysical characteristics, such as membrane binding properties. Thus, attachment of half-life extenders to peptides not only affects the pharmacokinetics but potentially also affects the pharmacodynamics. For example, peptide-stimulated internalization can lower the density of receptors at the cell surface, resulting in a loss of efficacy. On the other hand, receptor-mediated internalization is a key step in transcytosis important for passage across endogenous barriers. Hence, an in-depth understanding of the properties mediated by different half-life extenders beyond pharmacokinetics can be applied to tailor *in vivo* actions of peptides.

In conclusion, the three half-life extenders, C16-γGlu, C18acid-γGlu, and PEG20, had different effects on *in vitro* actions of PYY_{3-36}, i.e., Y_2R signaling, peptide-stimulated endocytosis, and membrane binding. We propose a temporal model for the control of Y_2R G_i-Arr3 signaling bias of PYY_{3-36} analogues based on receptor k_{off} rates and the relative speed difference by which Y_2R activates G_i and recruits Arr3. PEGylation of PYY_{3-36} position 7 increased the Y_2R k_{off} rate, which led to a size-dependent bias of Y_2R signaling toward G_i activity through a reduction of Arr3 recruitment potency. PEGylation also reduced membrane binding compared to either of the lipidation tags, with potential impact on the Y_2R binding dynamics. As a consequence of increased k_{off} rates and the subsequent reductions in Arr3 recruitment potencies, PEGylation of PYY_{3-36} resulted in minimal receptor internalization. In contrast to PEGylation, lipidation of PYY_{3-36} position 7 did not alter Y_2R k_{off} rates. Addition of C16-γGlu in position 7 of PYY_{3-36} had a negligible impact on Y_2R binding, Y_2R k_{off}, and Y_2R signaling. Thus, C16-γGlu had a negligible impact on endocytosis. Similarly, lipidating position 7 with C18acid-γGlu did not impact Y2R binding, Y_2R k_{off}, or Y_2R signaling. However, C18acid-γGlu minimized Y_2R-mediated internalization. Interestingly, this indicated that C18acid-γGlu decreased internalization through a non-arrestin-related mechanism. Furthermore, C18acid-γGlu did not increase the membrane binding of a PYY_{3-36} analogue compared to its backbone, unlike C16-γGlu which significantly increased membrane binding. Thus, we demonstrated how small structural changes in the lipid half-life extender could greatly influence internalization and membrane binding, with potential applicability for the development of nonadhering, noninternalizing peptide pharmaceuticals. We further observed how the site of lipidation was important for PYY_{3-36}'s Y_2R binding, signaling, and internalization. Thus, the composition of the lipid, its positioning, and the nature of the peptide are likely to affect the final impact of the half-life extender. This further emphasizes how half-life extenders can be applied to tailor properties beyond pharmacokinetics.

■ ASSOCIATED CONTENT

Supporting Information

The Supporting Information is available free of charge on the ACS Publications website at DOI: 10.1021/acs.molpharmaceut.9b00554.

Y2R activity data on fluorescently tagged peptides, supporting figures, details on peptide synthesis and purification, peptide chromatograms, and scripts applied for data analysis of live-cell imaging data as well as liposome intensity extraction (PDF)

■ AUTHOR INFORMATION

Corresponding Authors

*E-mail: slp@gubra.dk. Phone: +4531522650.
*E-mail: abeck-sickinger@uni-leipzig.de. Phone: +493419736900.
*E-mail: kjj@chem.ku.dk. Phone: +4535332430.

ORCID

Annette G. Beck-Sickinger: 0000-0003-4560-8020
Knud J. Jensen: 0000-0003-3525-5452

Notes

The authors declare no competing financial interest.

■ REFERENCES

(1) Batterham, R. L.; Cowley, M. A.; Small, C. J.; Herzog, H.; Cohen, M. A.; Dakin, C. L.; Wren, A. M.; Brynes, A. E.; Low, M. J.; Ghatei, M. A.; et al. Gut Hormone PYY3−36 Physiologically Inhibits Food Intake. *Nature* **2002**, *418* (8), 650−654.

(2) Batterham, R. L.; Cohen, M. A.; Ellis, S. M.; Le Roux, C. W.; Withers, D. J.; Frost, G. S.; Ghatei, M. A.; Bloom, S. R. Inhibition of Food Intake in Obese Subjects by Peptide YY3−36. *N. Engl. J. Med.* **2003**, *349* (10), 941−948.

(3) Walther, C.; Mörl, K.; Beck-Sickinger, A. G. Neuropeptide Y Receptors: Ligand Binding and Trafficking Suggest Novel Approaches in Drug Development. *J. Pept. Sci.* **2011**, *17* (4), 233−246.

(4) Holzer, P.; Reichmann, F.; Farzi, A. Neuropeptide Y. Peptide YY and Pancreatic Polypeptide in the Gut-Brain Axis. *Neuropeptides* **2012**, *46*, 261−274.

(5) Manning, S.; Batterham, R. L. The Role of Gut Hormone Peptide YY in Energy and Glucose Homeostasis: Twelve Years On. *Annu. Rev. Physiol.* **2014**, *76* (1), 585−608.

(6) Østergaard, S.; Wulff, B. S.; Frieboes, K. W. C.; Wieczorek, B. Selective PYY Compounds and Uses Thereof. WO 2016/124687 A1, 2016.

(7) Bloom, S. R. Peptide YY (PYY) Analogues. WO 2015/177573A1, 2015.

(8) Kofoed, J.; Ynddal, L.; Østergaard, S.; Jørgensen, R.; Nielsen, F. S.; Nilsson, C.; Thomsen, J. K. Long-Acting Y2 Receptor Agonists. WO 2011/058165A1, 2011.

(9) Macielag, M.; Patch, R. J.; Zhang, R.; Case, M. A.; Wall, M.; Zhang, Y.-M. Cyclic Peptide Tyrosine Tyrosine Compounds as

DOI: 10.1021/acs.molpharmaceut.9b00554
Mol. Pharmaceutics 2019, 16, 3665−3677

Modulators of Neuropeptide Y Receptors. WO 2018/081367 A1, 2018.
(10) Østergaard, S.; Kofoed, J.; Paulsson, J. F.; Madsen, K. G.; Jorgensen, R.; Wulff, B. S. Design of Y2 Receptor Selective and Proteolytically Stable PYY3−36 Analogues. *J. Med. Chem.* **2018**, *61*, 10519−10530.
(11) Niida, A.; Kanematsu-Yamaki, Y.; Asakawa, T.; Ishimura, Y.; Fujita, H.; Matsumiya, K.; Nishizawa, N.; Adachi, Y.; Mochida, T.; Tsuchimori, K.; et al. Antiobesity and Emetic Effects of a Short-Length Peptide YY Analog and Its PEGylated and Alkylated Derivatives. *Bioorg. Med. Chem.* **2018**, *26* (3), 566−572.
(12) De Silva, A.; Bloom, S. R. Gut Hormones and Appetite Control: A Focus on PYY and GLP-1 as Therapeutic Targets in Obesity. *Gut Liver* **2012**, *6* (1), 10−20.
(13) Ballantyne, G. H. Peptide YY(1−36) and Peptide YY(3−36): Part II. Changes after Gastrointestinal Surgery and Bariatric Surgery - Part. I. Distribution, Release and Actions. *Obes. Surg.* **2006**, *16* (6), 795−803.
(14) Olsen, J.; Kofoed, J.; Ostergaard, S.; Wulff, B. S.; Nielsen, F. S.; Jorgensen, R. Metabolism of Peptide YY 3−36 in Gottingen Mini-Pig and Rhesus Monkey. *Peptides* **2016**, *78*, 59−67.
(15) le Roux, C. W.; Borg, C. M.; Murphy, K. G.; Vincent, R. P.; Ghatei, M. A.; Bloom, S. R. Supraphysiological Doses of Intravenous PYY3−36 Cause Nausea, but No Additional Reduction in Food Intake. *Ann. Clin. Biochem.* **2008**, *45* (1), 93−95.
(16) van Witteloostuijn, S. B.; Pedersen, S. L.; Jensen, K. J. Half-Life Extension of Biopharmaceuticals Using Chemical Methods: Alternatives to PEGylation. *ChemMedChem* **2016**, *11* (22), 2474−2495.
(17) Bech, E. M.; Pedersen, S. L.; Jensen, K. J. Chemical Strategies for Half-Life Extension of Biopharmaceuticals: Lipidation and Its Alternatives. *ACS Med. Chem. Lett.* **2018**, *9* (7), 577−580.
(18) Ehrlich, G. K.; Michel, H.; Truitt, T.; Riboulet, W.; Pop-Damkov, P.; Goelzer, P.; Hainzl, D.; Qureshi, F.; Lueckel, B.; Danho, W.; et al. Preparation and Characterization of Albumin Conjugates of a Truncated Peptide YY Analogue for Half-Life Extension. *Bioconjugate Chem.* **2013**, *24* (12), 2015−2024.
(19) Ortiz, A. a; Milardo, L. F.; DeCarr, L. B.; Buckholz, T. M.; Mays, M. R.; Claus, T. H.; Livingston, J. N.; Mahle, C. D.; Lumb, K. J. A Novel Long-Acting Selective Neuropeptide Y2 Receptor Polyethylene Glycol-Conjugated Peptide Agonist Reduces Food Intake and Body Weight and Improves Glucose Metabolism in Rodents. *J. Pharmacol. Exp. Ther.* **2007**, *323* (2), 692−700.
(20) Madsen, K.; Knudsen, L. B.; Agersoe, H.; Nielsen, P. F.; Thøgersen, H.; Wilken, M.; Johansen, N. L. Structure-Activity and Protraction Relationship of Long-Acting Glucagon-like Peptide-1 Derivatives: Importance of Fatty Acid Length, Polarity, and Bulkiness. *J. Med. Chem.* **2007**, *50* (24), 6126−6132.
(21) Evers, A.; Bossart, M.; Pfei, S.; Elvert, R.; Schreuder, H.; Kurz, M.; Stengelin, S.; Lorenz, M.; Herling, A.; Konkar, A.; et al. Dual Glucagon-like Peptide 1 (GLP-1)/Glucagon Receptor Agonists Specifically Optimized for Multidose Formulations. *J. Med. Chem.* **2018**, *61*, 5580.
(22) Secher, A.; Jelsing, J.; Baquero, A. F.; Hecksher-Sørensen, J.; Cowley, M. A.; Dalbøge, L. S.; Hansen, G.; Grove, K. L.; Pyke, C.; Raun, K.; et al. The Arcuate Nucleus Mediates GLP-1 Receptor Agonist Liraglutide-Dependent Weight Loss. *J. Clin. Invest.* **2014**, *124* (10), 4473−4488.
(23) Castelletto, V.; Hamley, I. W.; Seitsonen, J.; Ruokolainen, J.; Harris, G.; Bellmann-Sickert, K.; Beck-Sickinger, A. G. Conformation and Aggregation of Selectively PEGylated and Lipidated Gastric Peptide Hormone Human PYY 3−36. *Biomacromolecules* **2018**, *19* (11), 4320−4332.
(24) Hutchinson, J. A.; Burholt, S.; Hamley, I. W.; Lundback, A.-K.; Uddin, S.; Gomes Dos Santos, A.; Reza, M.; Seitsonen, J.; Ruokolainen, J. The Effect of Lipidation on the Self-Assembly of the Gut-Derived Peptide Hormone PYY 3−36. *Bioconjugate Chem.* **2018**, *29* (7), 2296−2308.
(25) Mäde, V.; Babilon, S.; Jolly, N.; Wanka, L.; Bellmann-Sickert, K.; Diaz Gimenez, L. E.; Mörl, K.; Cox, H. M.; Gurevich, V. V.; Beck-Sickinger, A. G. Peptide Modifications Differentially Alter G Protein-Coupled Receptor Internalization and Signaling Bias. *Angew. Chem., Int. Ed.* **2014**, *53* (38), 10067−10071.
(26) Jensen, K. J.; Shelton, P. T.; Pedersen, S. L. In *Peptide Synthesis and Application*, 2nd ed.; Walker, J. M., Ed.; Humana Press: Hatfield, U.K., 2013.
(27) Böhme, I.; Stichel, J.; Walther, C.; Mörl, K.; Beck-Sickinger, A. G. Agonist Induced Receptor Internalization of Neuropeptide Y Receptor Subtypes Depends on Third Intracellular Loop and C-Terminus. *Cell. Signalling* **2008**, *20* (10), 1740−1749.
(28) Wanka, L.; Babilon, S.; Kaiser, A.; Mörl, K.; Beck-Sickinger, A. G. Different Mode of Arrestin-3 Binding at the Human Y1 and Y2 Receptor. *Cell. Signalling* **2018**, *50* (May), 58−71.
(29) Kaiser, A.; Hempel, C.; Wanka, L.; Schubert, M.; Hamm, H. E.; Beck-Sickinger, A. G. G Protein Preassembly Rescues Efficacy of W 6.48 Toggle Mutations in Neuropeptide Y2 Receptor. *Mol. Pharmacol.* **2018**, *93*, 387−401.
(30) Dawaliby, R.; Trubbia, C.; Delporte, C.; Noyon, C.; Ruysschaert, J. M.; Van Antwerpen, P.; Govaerts, C. Phosphatidylethanolamine Is a Key Regulator of Membrane Fluidity in Eukaryotic Cells. *J. Biol. Chem.* **2016**, *291* (7), 3658−3667.
(31) Stella, S.; Mesa, P.; Thomsen, J.; Paul, B.; Alcón, P.; Jensen, S. B.; Saligram, B.; Moses, M. E.; Hatzakis, N. S.; Montoya, G. Conformational Activation Promotes CRISPR-Cas12a Catalysis and Resetting of the Endonuclease Activity. *Cell* **2018**, *175*, 1856−1871.
(32) Hatzakis, N. S.; Bhatia, V. K.; Larsen, J.; Madsen, K. L.; Bolinger, P.; Kunding, A. H.; Castillo, J.; Gether, U.; Hedegård, P.; Stamou, D. How Curved Membranes Recruit Amphipathic Helices and Protein Anchoring Motifs. *Nat. Chem. Biol.* **2009**, *5* (11), 835−841.
(33) Jonassen, I.; Havelund, S.; Hoeg-Jensen, T.; Steensgaard, D. B.; Wahlund, P. O.; Ribel, U. Design of the Novel Protraction Mechanism of Insulin Degludec, an Ultra-Long-Acting Basal Insulin. *Pharm. Res.* **2012**, *29* (8), 2104−2114.
(34) Lau, J.; Bloch, P.; Schäffer, L.; Pettersson, I.; Spetzler, J.; Kofoed, J.; Madsen, K.; Knudsen, L. B.; McGuire, J.; Steensgaard, D. B.; et al. Discovery of the Once-Weekly Glucagon-Like Peptide-1 (GLP-1) Analogue Semaglutide. *J. Med. Chem.* **2015**, *58* (18), 7370−7380.
(35) van Witteloostuijn, S. B.; Mannerstedt, K.; Wismann, P.; Bech, E. M.; Thygesen, M. B.; Vrang, N.; Jelsing, J.; Jensen, K. J.; Pedersen, S. L. Neoglycolipids for Prolonging the Effects of Peptides: Self-Assembling Glucagon-like Peptide 1 Analogues with Albumin Binding Properties and Potent in Vivo Efficacy. *Mol. Pharmaceutics* **2017**, *14*, 193−205.
(36) Nygaard, R.; Nielbo, S.; Schwartz, T. W.; Poulsen, F. M. The PP-Fold Solution Structure of Human Polypeptide YY and Human PYY3−36 as Determined by NMR. *Biochemistry* **2006**, *45* (27), 8350−8357.
(37) Rajagopal, S.; Rajagopal, K.; Lefkowitz, R. J. Teaching Old Receptors New Tricks: Biasing Seven-Transmembrane Receptors. *Nat. Rev. Drug Discovery* **2010**, *9* (May), 373−386.
(38) Walther, C.; Nagel, S.; Gimenez, L. E.; Mörl, K.; Gurevich, V. V.; Beck-Sickinger, A. G. Ligand-Induced Internalization and Recycling of the Human Neuropeptide Y2 Receptor Is Regulated by Its Carboxyl-Terminal Tail. *J. Biol. Chem.* **2010**, *285* (53), 41578−41590.
(39) Wacker, D.; Wang, S.; McCorvy, J. D.; Betz, R. M.; Venkatakrishnan, A. J.; Levit, A.; Lansu, K.; Schools, Z. L.; Che, T.; Nichols, D. E.; et al. Crystal Structure of an LSD-Bound Human Serotonin Receptor. *Cell* **2017**, *168*, 377−389.
(40) Choi, I. Y.; Park, S. H.; Trautmann, M.; Moon, M. J.; Kim, J. Y.; Lee, Y. M.; Hompesch, M.; Kwon, S. C. Underlying Superagonistic Mechanisms of Efpeglenatide in Glycaemic Control and Weight Loss Potency. In *American Diabetes Association's (ADA) 76th Scientific Sessions*; New Orleans, LA, 2016; pp 1068-P.
(41) Jones, B.; Buenaventura, T.; Kanda, N.; Chabosseau, P.; Owen, B. M.; Scott, R.; Goldin, R.; Angkathunyakul, N.; Corrêa, I. R.; Bosco,

DOI: 10.1021/acs.molpharmaceut.9b00554
Mol. Pharmaceutics 2019, 16, 3665−3677

D.; et al. Targeting GLP-1 Receptor Trafficking to Improve Agonist Efficacy. *Nat. Commun.* **2018**, *9* (1), 1−17.
(42) Tsuji, M.; Ueda, S.; Hirayama, T.; Okuda, K.; Sakaguchi, Y.; Isono, A.; Nagasawa, H. FRET-Based Imaging of Transbilayer Movement of Pepducin in Living Cells by Novel Intracellular Bioreductively Activatable Fluorescent Probes. *Org. Biomol. Chem.* **2013**, *11* (18), 3030.
(43) Covic, L.; Misra, M.; Badar, J.; Singh, C.; Kuliopulos, A. Pepducin-Based Intervention of Thrombin-Receptor Signaling and Systemic Platelet Activation. *Nat. Med.* **2002**, *8* (10), 1161−1165.
(44) Trier, S.; Linderoth, L.; Bjerregaard, S.; Andresen, T. L.; Rahbek, U. L. *PLoS One* **2014**, *9* (10), e109939.
(45) Shpilman, M.; Niv-Spector, L.; Katz, M.; Varol, C.; Solomon, G.; Ayalon-Soffer, M.; Boder, E.; Halpern, Z.; Elinav, E.; Gertler, A. Development and Characterization of High Affinity Leptins and Leptin Antagonists. *J. Biol. Chem.* **2011**, *286* (6), 4429−4442.
(46) Oh, D.; Shirazi, A. N.; Northup, K.; Sullivan, B.; Tiwari, R. K.; Biso, M.; Parang, K. Enhanced Cellular Uptake of Short Polyarginine Peptides through Fatty Acylation and Cyclization. *Mol. Pharmaceutics* **2014**, *11*, 2845−2854.
(47) Zerbe, O.; Neumoin, A.; Mares, J.; Walser, R.; Zou, C. Recognition of Neurohormones of the NPY Family by Their Receptors. *J. Recept. Signal Transduction Res.* **2006**, *26* (5−6), 487−504.
(48) Lerch, M.; Mayrhofer, M.; Zerbe, O. Structural Similarities of Micelle-Bound Peptide YY (PYY) and Neuropeptide Y (NPY) Are Related to Their Affinity Profiles at the Y Receptors. *J. Mol. Biol.* **2004**, *339* (5), 1153−1168.
(49) Schwyzer, R. Peptide-Membrane Interactions and a New Principle in Quantitative Structure-Activity Relationships. *Biopolymers* **1991**, *31* (6), 785−792.
(50) Pasut, G.; Veronese, F. M. State of the Art in PEGylation: The Great Versatility Achieved after Forty Years of Research. *J. Controlled Release* **2012**, *161* (2), 461−472.
(51) Peterson, Y. K.; Luttrell, L. M. The Diverse Roles of Arrestin Scaffolds in G Protein-Coupled Receptor Signaling. *Pharmacol. Rev.* **2017**, *69* (3), 256−297.
(52) Ouedraogo, M.; Lecat, S.; Rochdi, M. D.; Hachet-Haas, M.; Matthes, H.; Gicquiaux, H.; Verrier, S.; Gaire, M.; Glasser, N.; Mély, Y.; et al. Distinct Motifs of Neuropeptide y Receptors Differentially Regulate Trafficking and Desensitization. *Traffic* **2008**, *9* (3), 305−324.
(53) Parker, S. L.; Kane, J. K.; Parker, M. S.; Berglund, M. M.; Lundell, I. A.; Li, M. D. Cloned Neuropeptide Y (NPY) Y1 and Pancreatic Polypeptide Y4 Receptors Expressed in Chinese Hamster Ovary Cells Show Considerable Agonist-Driven Internalization, in Contrast to the NPY Y2 Receptor. *Eur. J. Biochem.* **2001**, *268* (4), 877−886.
(54) Gicquiaux, H.; Lecat, S.; Gaire, M.; Dieterlen, A.; Me, Y.; Takeda, K.; Bucher, B.; Galzi, J. Rapid Internalization and Recycling of the Human Neuropeptide Y Y 1 Receptor. *J. Biol. Chem.* **2002**, *277* (8), 6645−6655.
(55) Berglund, M. M.; Schober, D. A.; Statnick, M. A.; McDonald, P. H.; Gehlert, D. R. The Use of Bioluminescence Resonance Energy Transfer 2 to Study Neuropeptide Y Receptor Agonist-Induced β-Arrestin 2 Interaction. *J. Pharmacol. Exp. Ther.* **2003**, *306* (1), 147−156.
(56) Lindner, D.; Walther, C.; Tennemann, A.; Beck-Sickinger, A. G. Functional Role of the Extracellular N-Terminal Domain of Neuropeptide Y Subfamily Receptors in Membrane Integration and Agonist-Stimulated Internalization. *Cell. Signalling* **2009**, *21* (1), 61−68.
(57) Lundell, I.; Bernhardt, N. R.; Johnsson, A.; Larhammar, D. Regulatory Peptides Internalization Studies of Chimeric Neuropeptide Y Receptors Y1 and Y2 Suggest Complex Interactions between Cytoplasmic Domains. *Regul. Pept.* **2011**, *168* (1−3), 50−58.
(58) Parker, S. L.; Parker, M. S.; Wong, Y. Y.; Sah, R.; Balasubramaniam, A.; Sallee, F. Importance of a N-Terminal Aspartate in the Internalization of the Neuropeptide Y Y2 Receptor. *Eur. J. Pharmacol.* **2008**, *594*, 26−31.
(59) Keire, D. A.; Kobayashi, M.; Solomon, T. E.; Reeve, J. R. Solution Structure of Monomeric Peptide YY Supports the Functional Significance of the PP-Fold. *Biochemistry* **2000**, *39* (32), 9935−9942.
(60) Xu, B.; Vasile, S.; Østergaard, S.; Paulsson, J. F.; Pruner, J.; Åqvist, J.; Wulff, B. S.; Gutiérrez-De-Terán, H.; Larhammar, D.; Ostergaard, S.; et al. Binding Mode of the Peptide YY Carboxyterminus to the Human Y2 Receptor. *Mol. Pharmacol.* **2018**, *93*, 323−334.
(61) Kaiser, A.; Müller, P.; Zellmann, T.; Scheidt, H. a.; Thomas, L.; Bosse, M.; Meier, R.; Meiler, J.; Huster, D.; Beck-Sickinger, A. G.; et al. Unwinding of the C-Terminal Residues of Neuropeptide Y Is Critical for Y 2 Receptor Binding and Activation. *Angew. Chem., Int. Ed.* **2015**, *54* (25), 7446−7449.
(62) Wacker, D.; Wang, S.; McCorvy, J. D.; Betz, R. M.; Venkatakrishnan, A. J.; Levit, A.; Lansu, K.; Schools, Z. L.; Che, T.; Nichols, D. E.; et al. Crystal Structure of an LSD-Bound Human Serotonin Receptor. *Cell* **2017**, *168* (3), 377−389.E12.
(63) Davies, M.; Thiman, M.; Kugler, A. Efpeglenatide: A Once Monthly GLP-1 RA in the Pipeline. *Austin J. Endocronology Diabetes* **2016**, *3* (4), 3−6.
(64) Misaki, R.; Morimatsu, M.; Uemura, T.; Waguri, S.; Miyoshi, E.; Taniguchi, N.; Matsuda, M.; Taguchi, T. Palmitoylated Ras Proteins Traffic through Recycling Endosomes to the Plasma Membrane during Exocytosis. *J. Cell Biol.* **2010**, *191* (1), 23−29.
(65) Kinlough, C. L.; Mcmahan, R. J.; Poland, P. A.; Bruns, J. B.; Harkleroad, K. L.; Stremple, R. J.; Kashlan, O. B.; Weixel, K. M.; Weisz, O. A.; Hughey, R. P. Recycling of MUC1 Is Dependent on Its Palmitoylation. *J. Biol. Chem.* **2006**, *281* (17), 12112−12122.
(66) Alhosaini, K.; Bahattab, O.; Qassam, H.; Challiss, R. A. J.; Willars, G. B. Ligand-Specific Signaling Profiles and Resensitization Mechanisms of the Neuromedin U2 Receptor. *Mol. Pharmacol.* **2018**, *94*, 674−688.
(67) Smith, J. S.; Rajagopal, S. The β-Arrestins: Multifunctional Regulators of G Protein-Coupled Receptors. *J. Biol. Chem.* **2016**, *291* (17), 8969−8977.
(68) Parker, M. S.; Sah, R.; Parker, S. L. Peptides Surface Masking Shapes the Traffic of the Neuropeptide Y Y2 Receptor. *Peptides* **2012**, *37* (1), 40−48.
(69) Irannejad, R.; Von Zastrow, M. GPCR Signaling along the Endocytic Pathway. *Curr. Opin. Cell Biol.* **2014**, *27* (1), 109−116.

DOI: 10.1021/acs.molpharmaceut.9b00554
Mol. Pharmaceutics 2019, 16, 3665−3677